An Interference to Noise Ratio Handover mechanism for Mobile Visible Light Communication Networks

Meysam Mayahi, Antonio Costanzo, Valeria Loscrì, Anna Vegni

An Interference to Noise Ratio Handover mechanism for Mobile Visible Light Communication Networks

Meysam Mayahi
Inria Lille - Nord Europe
meysam.mayahi@inria.fr

Antonio Costanzo
Inria Lille - Nord Europe
antonio.costanzo@inria.fr

Valeria Loscrí
Inria Lille - Nord Europe
valeria.loscri@inria.fr

Anna Maria Vegni
Roma Tre University
annamaria.vegni@uniroma3.it

***Abstract*—Visible Light Communication (VLC) is recognized as a complement communication technology that meets many hurdles of Radio Frequency (RF) systems. For example, VLC overcomes the limited RF spectrum resources for mobile users, even though its application demands an effective mechanism to handover among the different devices, in order to keep the connectivity consistent. In this paper, a new handover mechanism is introduced for mobile VLC nodes, based on a real time evaluation of the Interference-to-Noise Ratio (INR). This mechanism is coupled with four adaptive modulation schemes to further enhance the data rate. The communication system is evaluated at 0.15 mps and 0.3 mps velocities for different parameters *i.e.*, handover rate, delivered data per handover and handover delay ratio, through an extensive simulated campaign. An experimental validation carried out through software-defined approach, considering a small-scale scenario and low power Light Emitting Diodes (LEDs). A perfect results alignment between simulation and measurement show how suggested INR-based mechanism overcomes classical SNR-based handover for all performance parameters evaluated in this study.**

***Index Terms*—Visible light communication, Interference-based handover, Adaptive Modulation Scheme.**

I. Introduction

Since a couple of decades, the spectrum crunch issue is encouraging the alternative solutions to meet the lack of sufficient radio resources for growing number of mobile devices and applications [1]. Among the others, Visible light Communication (VLC) is considered as a reliable complement to RF technologies not only because of the exploitation of the existing lighting infrastructures but also because of the potential availability of the huge optical spectrum [2]. On the other hand, the presence of the Line of Sight (LoS) between the transmitters (*i.e.*, Light Emitting Diodes - LEDs) and the receivers (*i.e.*, Photo Diodes - PD, or cameras) seems mandatory in most of applications [3].

The main challenge for the LoS requirement is the mobility, where the mobile receiver in VLC has to maintain a high-speed connection in uninterrupted manner within the coverage area of a single access point (AP), as well as when it is moving across multiple transmitters [2]. The principal solution for switching the communication session from one AP to another is the *handover mechanism*. The handover procedures are generally pushed by the degradation of the quality of the current link, followed by the selection of a higher quality host link (if there is any), and finally executing the handover through exchanging control packets among the nodes that share the link [4]. The link quality evaluation is determined by the error probability ratio, which follows the distribution of the link disturbances such as noise and interference [5].

Back to the VLC literature, the maximum received power indicators, such as the signal-to-noise ratio (SNR) with Gaussian noise distribution are the well-known link quality metrics, even though overhearing the disturbances from other VLC transmitters offer less accurate performance evaluation. In [6], the maximum received power has been used to make soft horizontal handover among coordinated multi-points (CoMP), by adjusting the handover power margin and time-to-trigger parameters. The received signal intensity (RSI) extension in [7] was inspired by the RF received signal strength (RSS) concept, and exploited in RSI-based handover technique for mobile VLC systems. Signal to interference and noise ratio (SINR) is used in [8] to manage vertical handover between Li-Fi and Wi-Fi and to reduce the handover rate through the concept of handover skipping. The SINR evaluates the communication link more precisely, specially when the noise and interference power levels are comparable. Consequently, the interference is modeled as a Gaussian random process too, with finite independent signal aggregation, where no individual signal dominates over the rest, [9]. At the same time, the scenarios where the disturbances are dominated by one or multiple sources are commonly present in VLC systems. When the power of individual interferer or accumulative interference is at least one order of magnitude larger than the noise, the system is interference dominant. In this case, INR ought to properly describe the interference distribution [5]. Nevertheless, the Quality of Service (QoS) constraints was exploited for handover management in hybrid RF/VLC indoor systems [10].

In this paper, INR is employed for the first time as a handover decision metric. Link quality analysis based on INR allows to identify the disturbance distribution, which can belong to two cases *i.e.*, • higher INR, which refers to an interference dominated scenario, and •• lower INR, where the noise and interference have similar strength and might be treated in the same way. An important parameter to be considered in interference dominated case is the Interferer-to-Interference Ratio (IIR), in order to verify the dominant interferer among all the interferers. Later on, the dominant interferer will be selected according to the application requirements in terms of reliability and stability of the communication system. Regarding the data rate, an additional improvement is obtained via adaptive modulation technique switching among On-Off Keying (OOK) and Pulse Shift Keying (PSK) with different modulation orders. The evaluation system is performed through extensive simulations based on NS3 simulator tool [11] and an experimental validation in a small-scale version scenario. The good match of the simulation and experiment results proves the faithful performance evaluation of the proposed handover and transmission mechanism.

The reminder of this paper is organised as follows: Section II presents the system model via algorithms and analytical description. The validation of the system model is presented in Section III by comparing the results of simulations and experimental testbed in different scenarios. Finally, conclusions are drawn at the end of the paper.

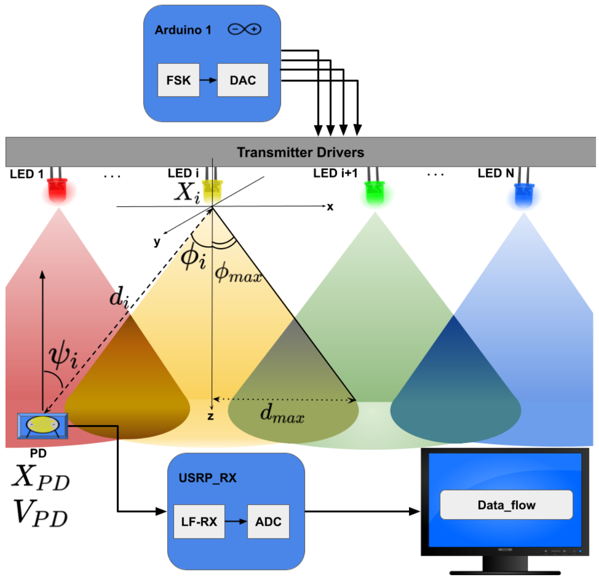

Fig. 1. Proposed VLC network architecture.

II. System model

In this section, we first describe the VLC propagation channel and the front-end model, then we will explain in detail the proposed handover mechanism. Consider the VLC system at Fig. 1 consisting of N transmitters and a receiver. At the generic transmitter i, the LED (fixed at position X_i) transforms the electrical signals to the light intensity in order to provide a background illumination along with visible light communication across the coverage area up to the maximum distance (*i.e.*, d_{max} [m]) depending on the half power semi-angle (*i.e.*, ϕ_{max}). Intensity modulation constrains the instantaneous output signal power $S_i(t)$ [W] between $P_{t,min}$ and $P_{t,max}$ with average optical signal power $P_{t,i} = E[S_i(t)]$. At the receiver side, for handover mechanism analysis purpose the photo diode (PD) assumes to move along the vector x with constant velocity V_{PD} and instantaneous position, X_{PD}. It generates an electric signal proportional to the average optical power received from LED i, $P_{r,i}$, estimated as:

$$P_{r,i} = h_{Lam,i} \cdot P_{t,i}, \tag{1}$$

where the channel impulse response between LED i and the PD (*i.e.*, $h_{Lam,i}$) is restricted to the Lambertian emission of order m *i.e.*,

$$h_{Lam,i} = \frac{(m+1)A}{2\pi d_i^2} \cos^m(\phi_i) T_s(\psi_i) g(\psi_i) \cos(\psi_i), \tag{2}$$

where A [cm^2] is the area of the PD which lays at distance d_i [m] far from the LED i, T_s and g are the gains of the PD optical filter and the optical concentrator, respectively at ϕ_i degree of radiance and ψ_i degree of acceptance angles.

In addition to the path loss, the VLC links suffers from the Additive White Gaussian Noise (AWGN) components including the thermal $\sigma_{thermal}$ and the shot noises σ_{shot}, which are expressed through a total contribution σ_n as:

$$\sigma_n^2 = \sigma_{shot}^2 + \sigma_{thermal}^2, \tag{3}$$

Given Gaussian noise dominant system, the performance of the link between transmitter i and the receiver is evaluated through the SNR_i expression *i.e.*,

$$SNR_i = \frac{(r \cdot P_{r,i})^2}{\sigma_n^2}, \tag{4}$$

where r [A/W] stands for PD responsivity

Interference in VLC systems arises when the PD detects the neighbour transmitter signals. A more precise link evaluation should consider both the interference and the background noise at the surrounding. Network interference is commonly modeled as a Gaussian distribution of independent processes with no signal prevailing [9]. In such scenarios, the central limit theorem is respected and the variance of the aggregate interference current (*i.e.*, σ_I^2 [A^2]) is used to define signal-to-interference ratio (SIR_i) evaluation of the link between LED i and the photo diode *i.e.*,

$$SIR_i = \frac{(r \cdot P_{r,i})^2}{\sigma_I^2}, \tag{5}$$

Performance evaluation of PD - LED i link when the disturbances from both noise and interference are in the same order of magnitude is feasible through $SINR_i$ *i.e.*,

$$SINR_i = \frac{(r \cdot P_{r,i})^2}{\sigma_I^2 + \sigma_n^2}, \tag{6}$$

The system is assumed to be interference dominant if the power of the interference is at least ten times larger than the noise power [5], then it is straightforward to define INR as a dominant disturbance identifier *i.e.*,

$$INR = \sum_{i=1}^{N} \frac{(r \cdot P_{r,i})^2}{\sigma_n^2}, \tag{7}$$

where N interferers are assumed to disturb each other.

Algorithm 1 Interference-based handover

Require: α, T_c, t_s
  measure INR
  while $INR \geq 10$ **do**
    measure IIR
    if $IIR \geq \beta$ **then**
      measure SNR_i
      if $SNR_i \geq \alpha$ **then**
        estimate t_c
        if $t_c \geq T_c$ **then**
          $T_c = t_c$
          candidate i
        end if
      end if
    end if
    $INR = INR - SNR_i$
  end while
  return T_c, i
  if null **then**
    backoff t_s
  end if

Algorithm 2 Adaptive Modulation Scheme

Require: i, α
  while $SNR_i \geq \alpha$ **do**
    adapt the modulation
    Transmit
    Receive
    measure SNR_i
  end while
  call handover

Gaussian interference assumption facilitates the link performance evaluation by employing the SNR_i, SIR_i and $SINR_i$ interchangeably. However this assumption is invalid in the presence of a dominant interferer. In such scenarios, the interference is properly modeled by the distribution of the dominant interferer [5]. In order to specify the dominant interferer, the IIR is calculated as:

$$IIR = \max_{i=1}^{N} \left(\frac{P_{r,i}}{\Sigma_i P_{r,i}} \right), \tag{8}$$

Low IIR fits well with the normal distribution assumption, while higher IIR proves less normal distribution and the Gaussian assumption leads to a heavier tail in the distribution. In extreme case when $IIR \rightarrow 1$, the only noticeable interference comes from a single dominant interferer. Finally, once the dominant disturbance of the system has been identified, the interference-based handover mechanisms relies on the appropriate metric in order to evaluate the link quality.

Algorithm 1 describes the main steps of INR-based handover mechanism. The mobile node (PD) in Fig. 1 is crossing multiple VLC coverage areas while moving along $x - axis$. The quality of the link degrades as it moves away from a fixed AP (LED i) due to the path loss and the front-end orientation. In order to maintain the connectivity link with a predefined Quality of Service (QoS) level, the receiver PD may assess the link quality frequently (*i.e.* every t_s seconds) and modify the transmission parameters, if required [12]. The INR-based algorithm evaluates the link performance based on the prominent component of the disturbances. To this end, it starts with INR calculation to determine if the system is noise-dominant or interference-dominant. In order to consider the system interference dominant, the interference power must be 10 times bigger than the noise power. In case that $INR < 10$, the noise and the interference power are comparable, and we treat them equally as a noise.

At the interference dominant system, there could be single or multiple dominant interferer. The IIR is able to identify the dominant interferer if IIR value is bigger than a threshold β, which is the minimum amount of IIR the system can detect and it is experimentally selected according to the node density(ρ_l). The interferers with $IIR \leq \beta$ are not dominant and are considered as a noise. The dominant interferer i with $IIR \geq \beta$ will be nominated for handover if it satisfies the QoS requirements of safety applications, expressed in terms of reliability and stability.
A reliable link has $SNR_i \geq \alpha$ [dB], where α is the minimum SNR level required for safety applications at maximum error probability, equal to 10^{-3} [13].
In order to increase the lifetime of a single link, the mobile node should avoid unnecessary handovers [14]. Skipping unstable VLC sessions will increase the connection time *i.e.*, t_c [s], estimated as

$$t_c = \frac{d_{max} + (X_{PD} - X_i)}{V_{PD}}, \tag{9}$$

Setting the minimum required connection time equal to T_c [s], the dominant interferer i will be candidate as AP if $INR_i \geq \alpha$ and $t_c \geq T_c$. This process will be successively reapplied in case of multiple dominant interferers. Finally, the dominant interferer i with the maximum connection time is returned to adaptive modulation scheme, as explained in Algorithm 2.

On top of handover mechanism, an Adaptive Modulation Scheme (ADM) protocol triggers different modulation schemes based on Table I, in order to obtain a proper compromise between the data rate and the communication robustness. The relative bitrates are appropriately selected at the simulator to cope with the testbed limited components. After co-channel interference mitigation among different LEDs using frequency division multiplexing [15], the proper modulation scheme is used for transmission, while the low SNR_i amount requires handover decision.

TABLE I
MODULATION TABLE

α [dB]	Modulation scheme (M)	Relative bitrate [kbps]	d_{max} [m]
11.14	OOK	100	0.2
11.3	4PSK	150	0.16
18.4	8PSK	200	0.12
20.6	16PSK	250	0.085

Algorithm 3 SNR-based handover

Require: α, T_c, t_s
  $SNR_{max} = \max_{i=1}^{N}\left(\frac{(rP_{r,i})^2}{\sigma_n^2}\right)$
  if $SNR \geq \alpha$ **then**
    estimate t_c
    if $t_c \geq T_c$ **then**
      $T_c = t_c$
      candidate i
    end if
  end if
  return T_c, i
  if null **then**
    backoff t_s
  end if

TABLE II
MAIN PARAMETERS

Parameter	Value[unit]
Responsivity, r	0.2 [A/W]
Area of PD , A	1.3 $[cm^2]$
Minimum Transmission time, T_c	200 [ms]
Sampling Time, t_i	100 [ms]
Half power semi-angle, ϕ_{max}	35°
Linear AP density, ρ_l	$[1, 10]$ [m^{-1}]
Minimum IIR, β	0.3
INR-based HO frame size	39 [Bytes]
SNR-based HO frame size	28 [Bytes]
Number of LEDs	5
Number of PDs	4
Input electrical power	1.0 [W]
Number of simulations	30
Duration of each simulation	100 [s]
Rounds of each simulation	10

III. VALIDATION

The proposed INR-based protocol for transmission and handover has been implemented in NS3 simulator [16] as well as a real specific scenario for proper experimental validation. In particular, we compare simulated and experimental protocol performance in terms of • handover rate, namely the number of successful handovers per minute, •• average delivered data per handover, namely the total delivered data over the total number of handover, and • • • handover delay ratio, namely the ratio between time required for performing the handover and total connection time.

In practice, we use an array of commercial low-power LEDs as APs, in order to build a small-scale setup. Each optical transmitter is connected to a dedicated output port of an Arduino 1 in order to control and drive separately each LED. A simple receiver consists of a low-cost PD and other passive elements is used for delivering the data to the signal process unity, mainly composed by a USRP 2920 and a Low Frequency daughterboard. The distance between the ceiling of the APs setup and the plane of the mobile receiver is constant, while the number of LEDs and the distance between them is properly modified to allow performance evaluation for different linear node densities (ρ_l).

As a benchmark, we model the SNR-based handover mechanism with the same parameters, and we compared both mechanisms in simulation and experimental tests. In the SNR-based case, the handover decision is based on the maximum received power and the connection time, while, for the sake of fairness, we applied the ADM on top of both handover mechanisms. Table II shows the main system parameters used in the simulation and experimental tests.

Assuming the testbed scenarios of Fig. 2, different configurations of LEDs represent different node's linear densities while feeding the signal to the USRP at different time interval manipulates different speeds. As the mobile node moves along the coverage area of a given AP, the SNR metric is used to measure the link QoS and allocate the modulation scheme for the next transmission bursts, whereas the interference is mitigated based on the frequency shift keying. When the error probability increases as a result of degradation of the link quality, the INR-based handover nominates an alternative

Fig. 2. Testbed configurations for performance evaluation, considering different ρ_l.

AP with the highest connection time. On the other hand the SNR-based algorithm is suggesting the link with the highest received power that last at least T_c seconds, otherwise it backs off the scanning for t_s seconds.

In Fig. 3, we compare the handover rate (*i.e.*, HO_{rate} $[min^{-1}]$) obtained with the INR-based and the SNR-based handover schemes, for different speeds. It can be shown that the handover rate has a reverse relationship with the average connection time $\overline{t_c}$ $[s]$ as follows:

$$HO_{rate} = \frac{60}{\overline{t_c}}, \qquad (10)$$

Regarding the excellent matching between the simulation and the testbed results, it is admitted that, on the same speed as the AP density increases, the SNR-based handover rate increases linearly. According to Eq. (9) and (10), going from lower to higher ρ_l, the distance between node PD (Rx) and node i (Tx) is decreasing. Since d_{max} and V_{PD} are fixed, the average connection time declines accordingly, and as a

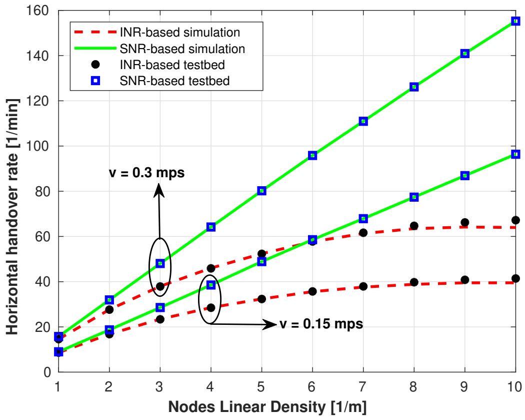

Fig. 3. Handover rate versus node density.

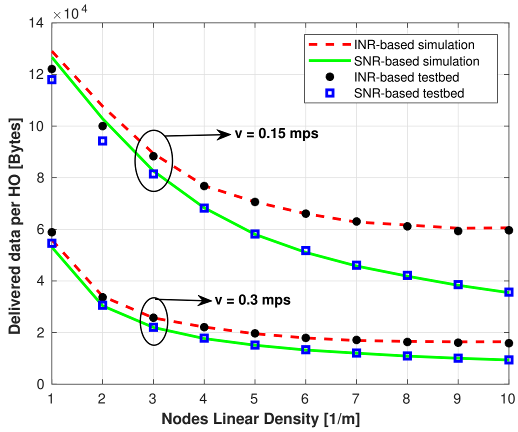

Fig. 4. Delivered data per handover versus node density.

result the handover rate increases. On the other side, the INR-based handover rate increases in the sparse AP deployment and saturates in the dense AP distribution. At the dense AP installation ($X_{PD} - X_i \leq d_{max}$) the longest t_c is determined by the farthest AP which stands at most d_{max} meter far from the mobile node. Higher velocity corresponds to the lower connection time, and hence higher handover rate.

In Fig. 4, we assess the impact of the node density on the average delivered data per handover at speed $0.3\ mps$ and $0.15\ mps$. In both medium access schemes, the transmission carried out when the front-end device is well covered by the AP (*i.e.*, $SNR \geq \alpha$). Giving t_c the available time for transmission, at rapid gait (*i.e.*, $0.3\ mps$) the connection time is shorter than the one of lower speed (*i.e.*, $0.15\ mps$) providing bigger portion of time for transmissions in different bitrate according to Table I. As a result, the average delivered data is larger for the higher speed than the lower one. It is also obvious from Fig. 4 that the INR-based mechanism always transmits more data per access point than the SNR-based scenario, that is not because of higher data rate obtained with our proposed scheme (*i.e.*, the transmission scheme is the same at both proposed scheme and the benchmark), but because the INR-based mechanism makes much less handovers for the same AP distribution. As the ρ_l increases the average delivered data decreases in both schemes with slight incline for INR-based scheme.

Regarding the handover delay, the time efficiency of a given handover mechanism is defined as the time required for performing the handover(HO_{delay}) to the whole connection time offered by that handover (t_c) [17] *i.e.*,

$$HO_{delay\ ratio} = \frac{\overline{HO_{delay}}}{\overline{t_c}} \times 100, \tag{11}$$

$$\overline{HO_{delay}} = \overline{t_{HO\ req}} + \overline{t_{HO\ res}}\ , \tag{12}$$

with $\overline{t_{HO\ req}}$ and $\overline{t_{HO\ res}}$ defined as the time necessary to • make an handover request and •• provide an handover response, respectively. Assuming the same frame size used for handover request and handover response (*i.e.*, $t_{HO\ req} = t_{HO\ res}$) included in the MAC frame format

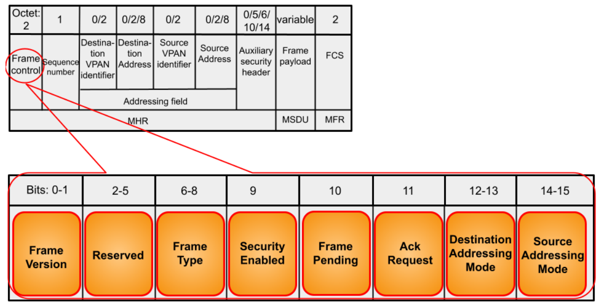

Fig. 5. General MAC frame 802.15.7 and the modified control field.

specified by IEEE standard for short-range wireless optical communication using VLC 802.15.7 [18], the reserved bits in the control frame of Fig. 5 is used to specify the velocity of the mobile node, as well as d_{max} of each LED rather than the number of interferers N for the INR-based mechanism. The required time to perform a handover is the handover frame size (*i.e.*, $HO_{frame\ size}$ [bits]) over the bitrate at both the transmitter and the receiver (*i.e.*, $\frac{1}{R_b(M)} = \frac{1}{R_{b,tx}(M)} + \frac{1}{R_{b,rx}(M)}$). Given the modulation scheme M ($M \in \{OOK, 4PSK, 8PSK, 16PSK\}$) and $R_{b,tx}(M) = R_{b,rx}(M)$ the handover request time is simplified through eq. (13),

$$t_{HO\ req}(M) = \frac{2\ HO_{frame\ size}}{R_{b,tx}(M)} \tag{13}$$

The average handover time is calculated as follows:

$$\overline{t_{HO\ req}} = \frac{\sum_M \left(t_{HO\ req}(M) \cdot HO_{rate}(M)\right)}{HO_{rate}}, \tag{14}$$

where $HO_{rate}(M)$ is the handover rate on the modulation scheme M. The evolution of the handover delay ratio comparing to AP density for different velocities is depicted in Fig. 6. At higher velocity, the connection time is lower resulting in less efficient handover delay ratio. For a given velocity, at the low density scenarios the SNR-based performs better due to the shorter handover frame size. As the node density increases, the number of SNR-based handover grows

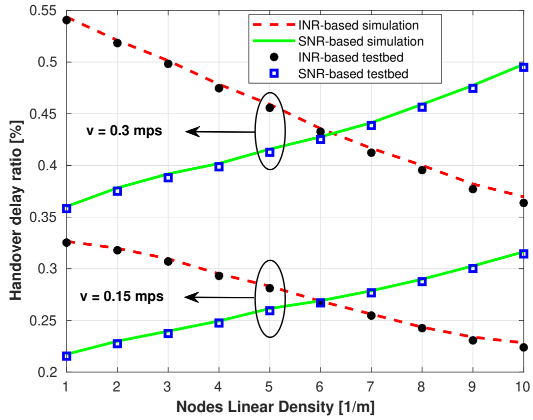

Fig. 6. Handover delay ratio versus node density.

linearly. Simultaneously, the dense AP deployment boost the received power at the front-end device which in return applies higher modulation levels and increases the bitrate, although the handover rate progresses faster than the bitrate, leading to $\frac{HO_{rate}}{R_b} \geq 1$. That is why the SNR-based handover delay ratio is monotonically increasing. On the other side, the interference-based handover mechanism substantially outperforms the SNR-based handover by recovering the higher overhead with the the lower HO_{rate}. The ratio $\frac{HO_{rate}}{R_b}$ in INR-based scheme is less than unity because the HO_{rate} reaches the saturation level at the high density, while the R_b continues increasing leading to decreasing delay ratio.

IV. Conclusions

A novel handover technique for mobile visible light communication nodes based on the INR and IIR is proposed and validated through the simulation and the experimental tests. A fair comparison between INR-based and SNR-based handover mechanisms is presented in terms of handover rate, average delivered data per handover, and handover delay ratio. The results in both simulation and experimental tests confirmed that the proposed algorithm avoids redundant handovers, and consequently, improves the average delivered data per handover, reducing significantly the overhead information of the network. At the same time, the handover delay ratio showed up to 1.5 times enhancement as compared to the SNR-based handover in high density scenarios (*i.e.*, $\rho_l = 10\ m^{-1}$).

Acknowledgment

This article is based on the work from COST Action NEWFOCUS CA19111, supported by COST (European Cooperation in Science and Technology).

References

[1] L.E.M. Matheus, A.B. Vieira, L.F.M. Vieira, M.A.M. Vieira and O. Gnawali, "Visible Light Communication: Concepts, Applications and Challenges," in IEEE Communications Surveys and Tutorials, vol. 21, no. 4, pp. 3204-3237, Fourthquarter 2019, doi: 10.1109/COMST.2019.2913348.

[2] H. Haas, L. Yin, Y. Wang and C. Chen, "What is LiFi?," in Journal of Lightwave Technology, vol. 34, no. 6, pp. 1533-1544, 15 March15, 2016, doi: 10.1109/JLT.2015.2510021.

[3] K. Cui, G. Chen, Z. Xu and R. D. Roberts, "Line-of-sight visible light communication system design and demonstration," 2010 7th International Symposium on Communication Systems, Networks and Digital Signal Processing (CSNDSP 2010), 2010, pp. 621-625, doi: 10.1109/CSNDSP16145.2010.5580360.

[4] Q. Dang and M. Yoo, "Handover Procedure and Algorithm in Vehicle to Infrastructure Visible Light Communication," in IEEE Access, vol. 5, pp. 26466-26475, 2017, doi: 10.1109/ACCESS.2017.2771199.

[5] M. Rahaim and T.D.C. Little, "Optical interference analysis in Visible Light Communication networks," 2015 IEEE International Conference on Communication Workshop (ICCW), 2015, pp. 1410-1415, doi: 10.1109/ICCW.2015.7247376.

[6] X. Wu, D.C. O'Brien, X. Deng and J.-P. M. G. Linnartz, "Smart Handover for Hybrid LiFi and WiFi Networks," in IEEE Transactions on Wireless Communications, vol. 19, no. 12, pp. 8211-8219, Dec. 2020, doi: 10.1109/TWC.2020.3020160.

[7] A.M. Vegni and T.D.C. Little, "Handover in VLC systems with cooperating mobile devices," 2012 International Conference on Computing, Networking and Communications (ICNC), 2012, pp. 126-130, doi: 10.1109/ICCNC.2012.6167395.

[8] M.S. Demir, H.B. Eldeeb and M. Uysal, "CoMP-Based Dynamic Handover for Vehicular VLC Networks," in IEEE Communications Letters, vol. 24, no. 9, pp. 2024-2028, Sept. 2020, doi: 10.1109/LCOMM.2020.2994416.

[9] M.Z. Win, P.C. Pinto and L.A. Shepp, "A Mathematical Theory of Network Interference and Its Applications," in Proceedings of the IEEE, vol. 97, no. 2, pp. 205-230, Feb. 2009, doi: 10.1109/JPROC.2008.2008764.

[10] M. Hammouda, S. Akın, A. M. Vegni, H. Haas and J. Peissig, "Link Selection in Hybrid RF/VLC Systems Under Statistical Queueing Constraints," in IEEE Transactions on Wireless Communications, vol. 17, no. 4, pp. 2738-2754, April 2018.

[11] G.F. Riley, T.R. Henderson (2010) The ns-3 Network Simulator. In: Wehrle K., Güneş M., Gross J. (eds) Modeling and Tools for Network Simulation. Springer, Berlin, Heidelberg. https://doi.org/10.1007/978-3-642-12331-3-2

[12] M. Mayahi, V. Loscrí, and A. Costanzo, "Link adaptive protocol for V2LC," in Proc. of the Workshop on Internet of Lights (IoL '21). ACM, New York, NY, USA, 13–17. DOI:https://doi.org/10.1145/3469264.3469807

[13] C. Song, "Performance Analysis of the IEEE 802.11p Multichannel MAC Protocol in Vehicular Ad Hoc Networks," Sensors 2017, 17, 2890. https://doi.org/10.3390/s17122890

[14] A.S. Sadiq, K.A. Bakar, K.Z. Ghafoor, *et al.* "An Intelligent Vertical Handover Scheme for Audio and Video Streaming in Heterogeneous Vehicular Networks," Mobile Network Applications 18, 879–895 (2013). https://doi.org/10.1007/s11036-013-0465-8

[15] A. Costanzo and V. Loscrí, "Visible Light Indoor Positioning in a Noise-aware Environment," in Proc. of 2019 IEEE Wireless Communications and Networking Conference (WCNC), 2019, pp. 1-6.

[16] A. Aldalbahi, M. Rahaim, A. Khreishah, M. Ayyash and T. D. C. Little, "Visible Light Communication Module: An Open Source Extension to the ns3 Network Simulator With Real System Validation," in IEEE Access, vol. 5, pp. 22144-22158, 2017, doi: 10.1109/ACCESS.2017.2759779.

[17] D.Q. Hien and M. Yoo, "Handover in outdoor Visible Light Communication system," in Proc. of 2017 International Conference on Information Networking (ICOIN), 2017, pp. 67-69, doi: 10.1109/ICOIN.2017.7899477.

[18] "IEEE Standard for Local and Metropolitan Area Networks–Part 15.7: Short-Range Wireless Optical Communication Using Visible Light," in IEEE Std 802.15.7-2011 , vol., no., pp.1-309, 6 Sept. 2011, doi: 10.1109/IEEESTD.2011.6016195.